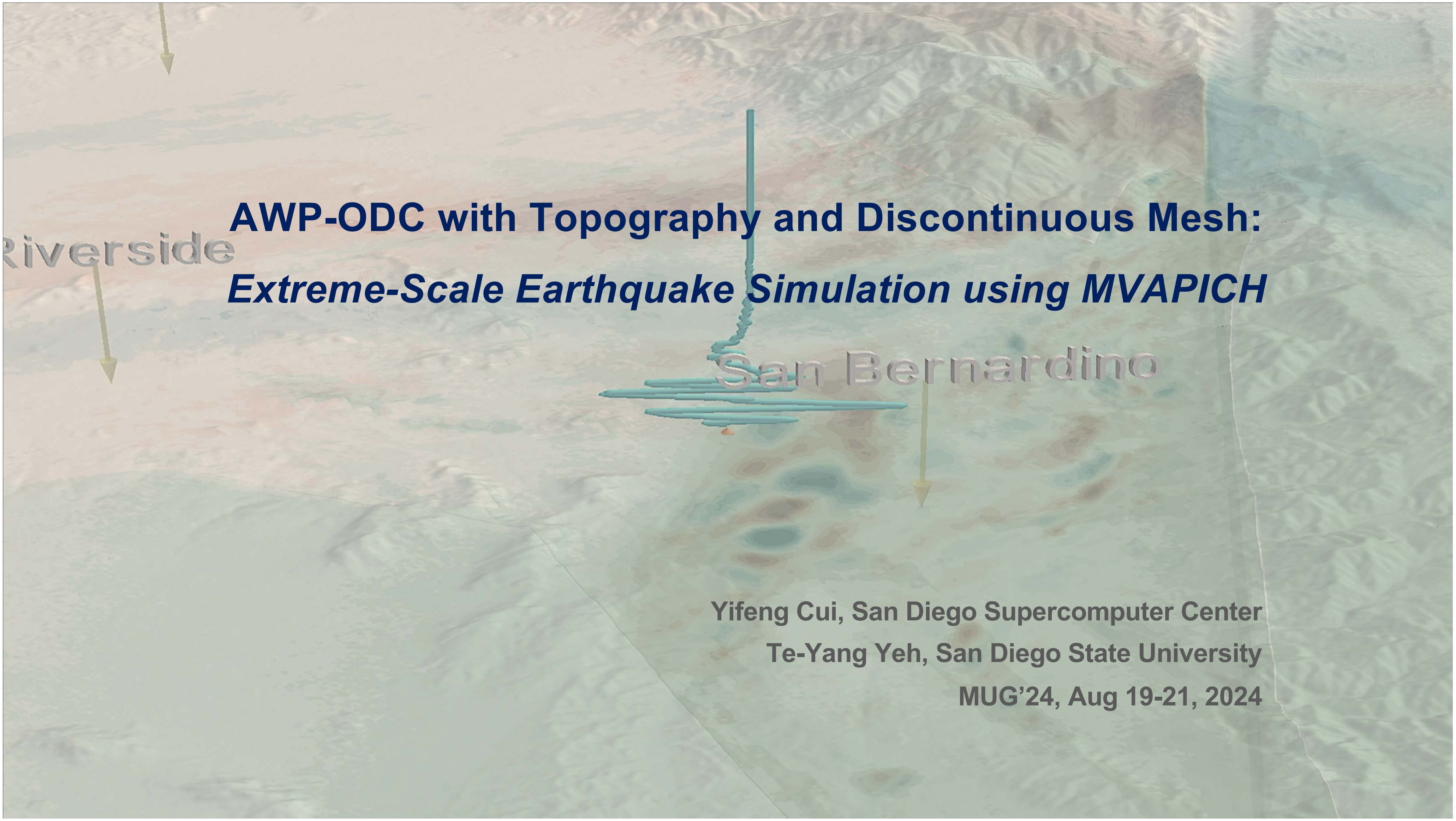

AWP-ODC with Topography and Discontinuous Mesh:

Extreme-Scale Earthquake Simulation using MVAPICH

Yifeng Cui, San Diego Supercomputer Center
Te-Yang Yeh, San Diego State University
MUG’24, Aug 19-21, 2024

Acknowledgments

HPGeoC Team

Akash Palla

Arnav Talreja

Daniel Roten

Collaborators

Philip Maechling

Ossian O'Reilly

Kim Olsen

Lars Koesterke

NOWLAB Team

DK Panda

Hari Subramoni

Qinghua Zhou

Lang Xu

Computing Allocation OLCF DD, TACC LSCP and CSA, ACCESS Delta, SDSC Expanse, AMD AAC, DOE INCITE & ALCC

Funding NSF CSSI, LCCF/CSA, NSF/USGS SCEC Core, SDSC

Advanced Earthquake Modeling with Nonlinearity and Topography in AWP-ODC

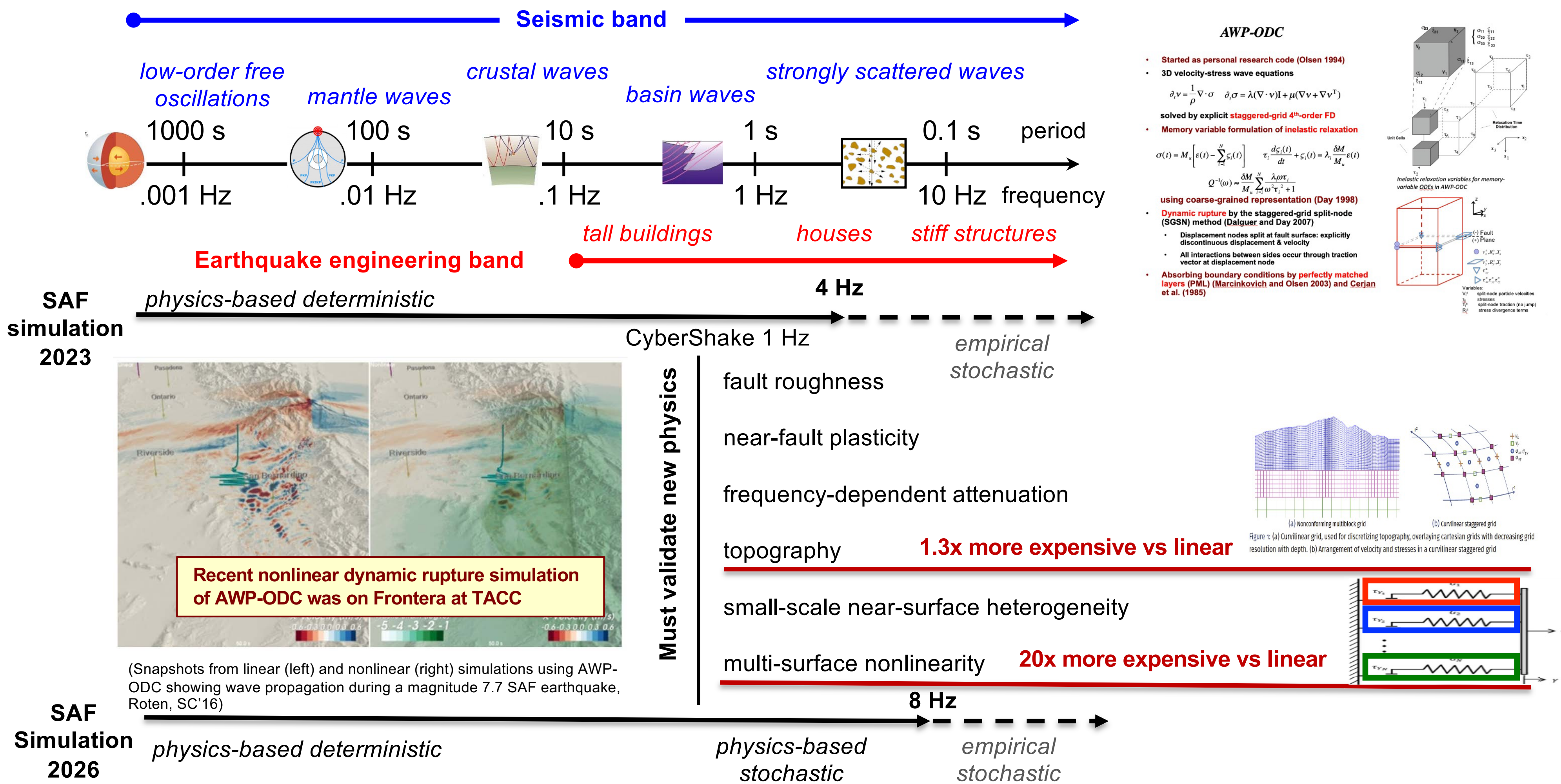

AWP-ODC Performance and MV2 Evaluation

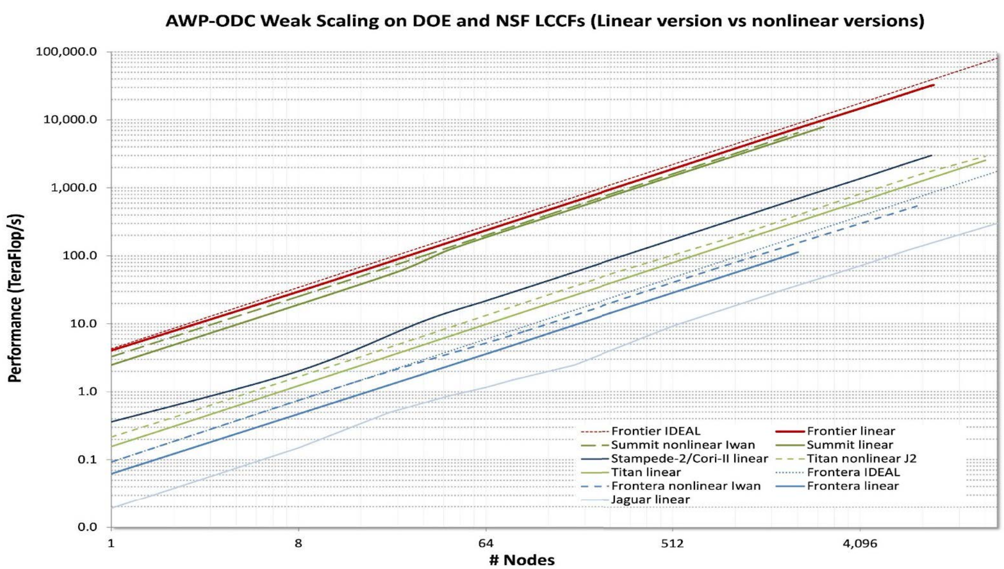

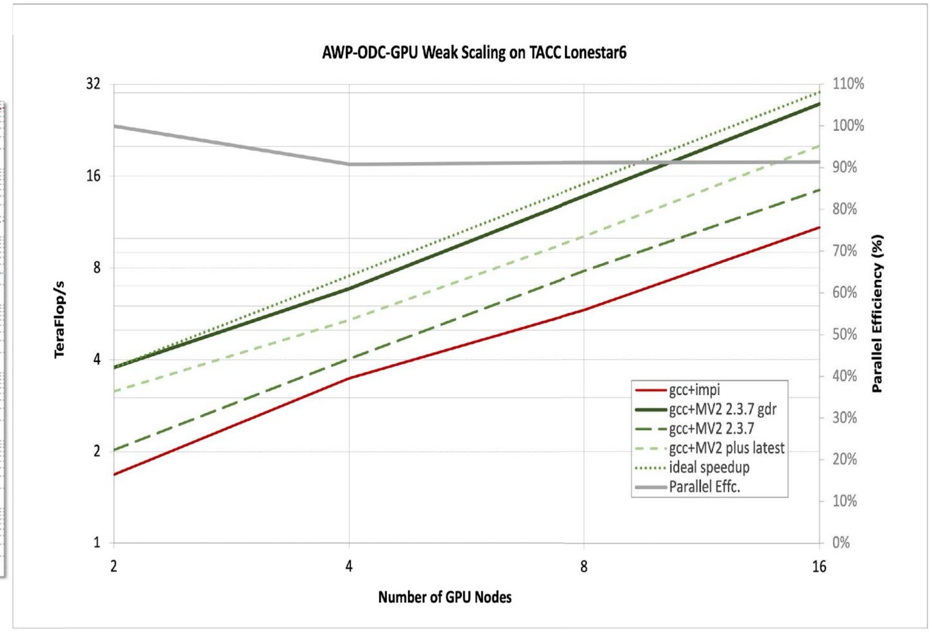

AWP-ODC simulation allocation annually ca. 200-300M core-hours in recent years, supported by DOE INCITE/ALCC and NSF LSCR (TACC) computing programs

AWP-ODC	K20X	KNL7250	V100 (NVLink)	A100 (NVLink) Openmpi	A100 (PCIe) impi	A100 (PCIe+Opt) MV2-gdr-MPC	H100 (PCIe)	H100 (PCIe+Opt)	MI250X (Slingshot)	GH200
MLUPS**	552	1092	1598	1937	896	2009	3713	5145	1711	8480
Speedup	1x*	1.98x	2.89x	3.51x	1.62x	3.64x	6.72x	9.32x	3.10x	15.36x

* 160x160x2048 per GPU configuration ** Millions of lattice point update completed per second

AWP-ODC-Topo Weak Scaling on Frontier

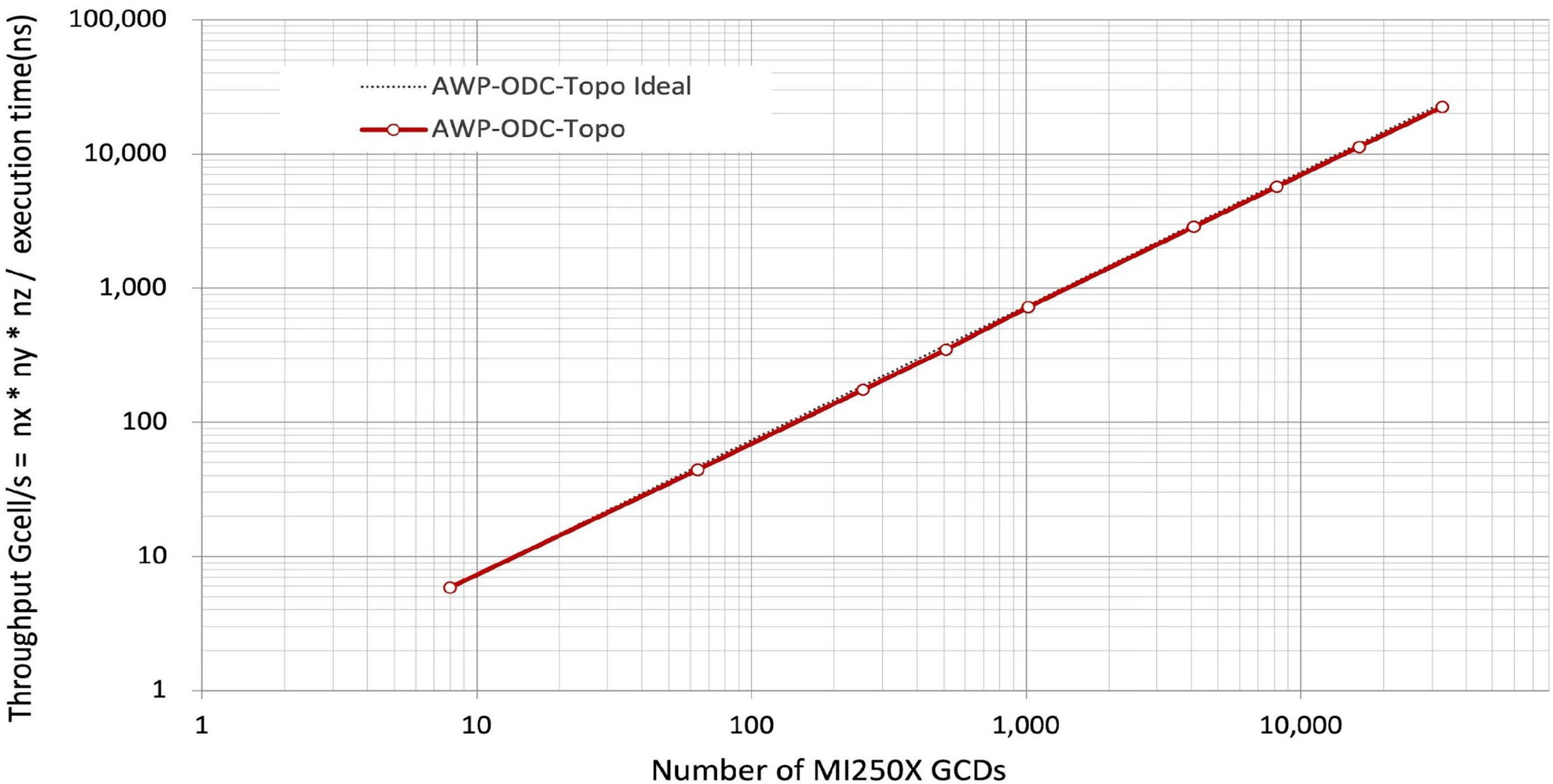

AWP-ODC-Topo w/ and w/o ROCm-Aware on Frontier

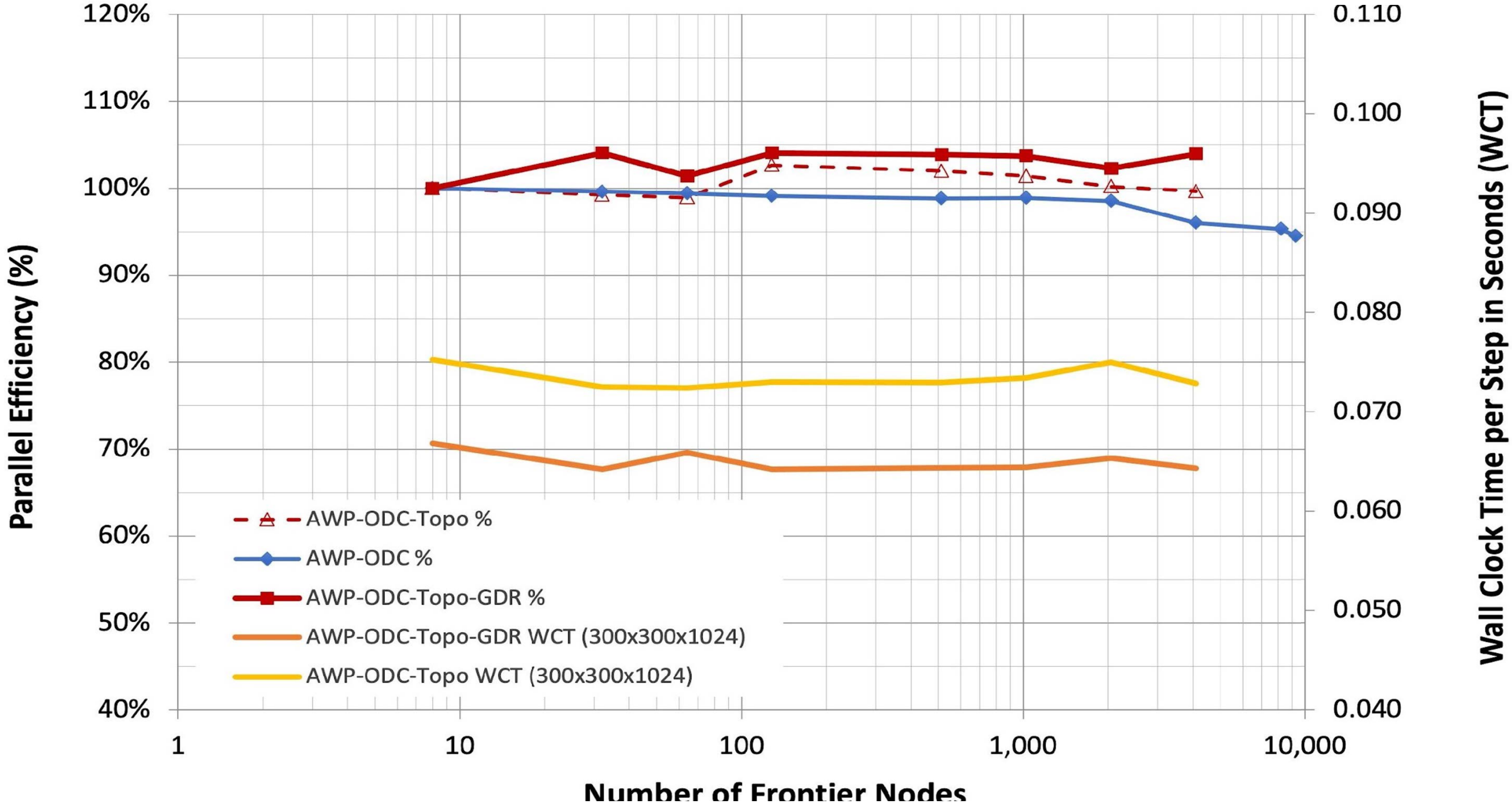

Computational Requirements of AWP-ODC

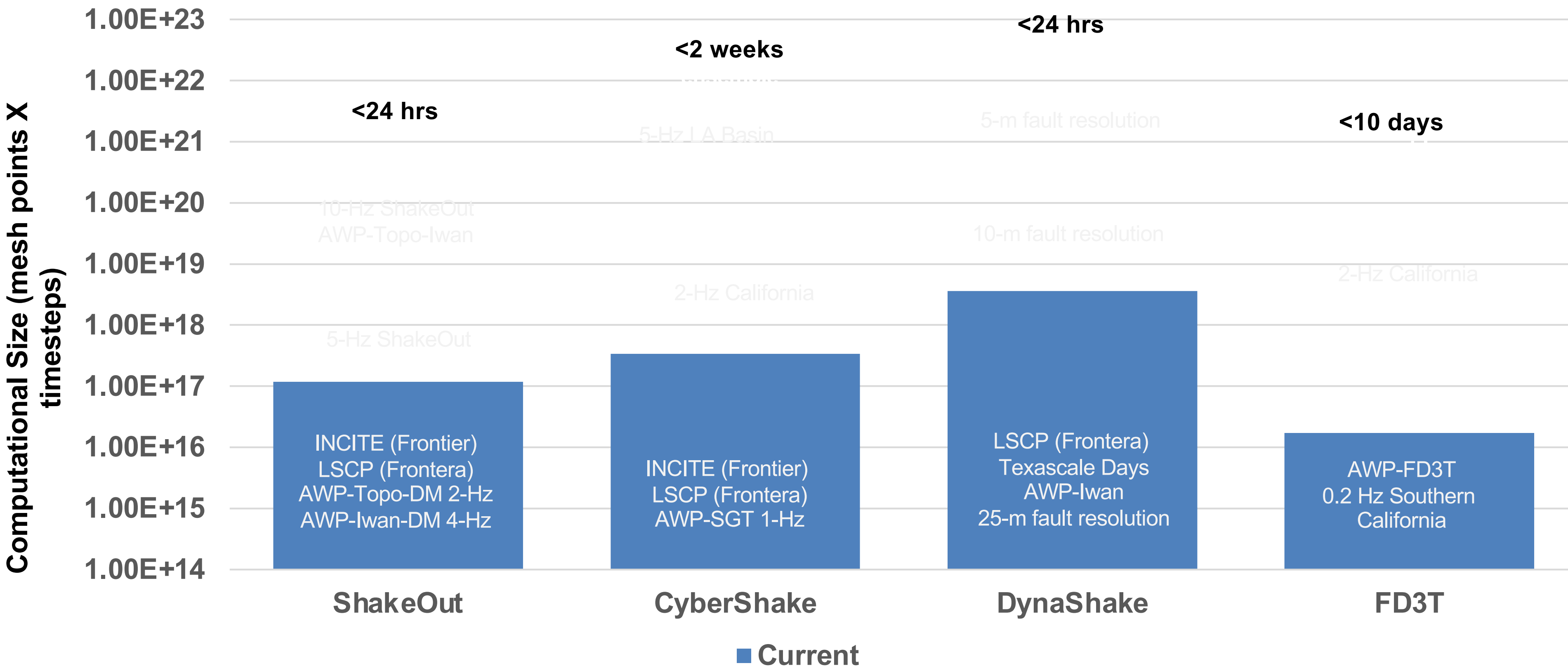

Computational Requirements of AWP-ODC

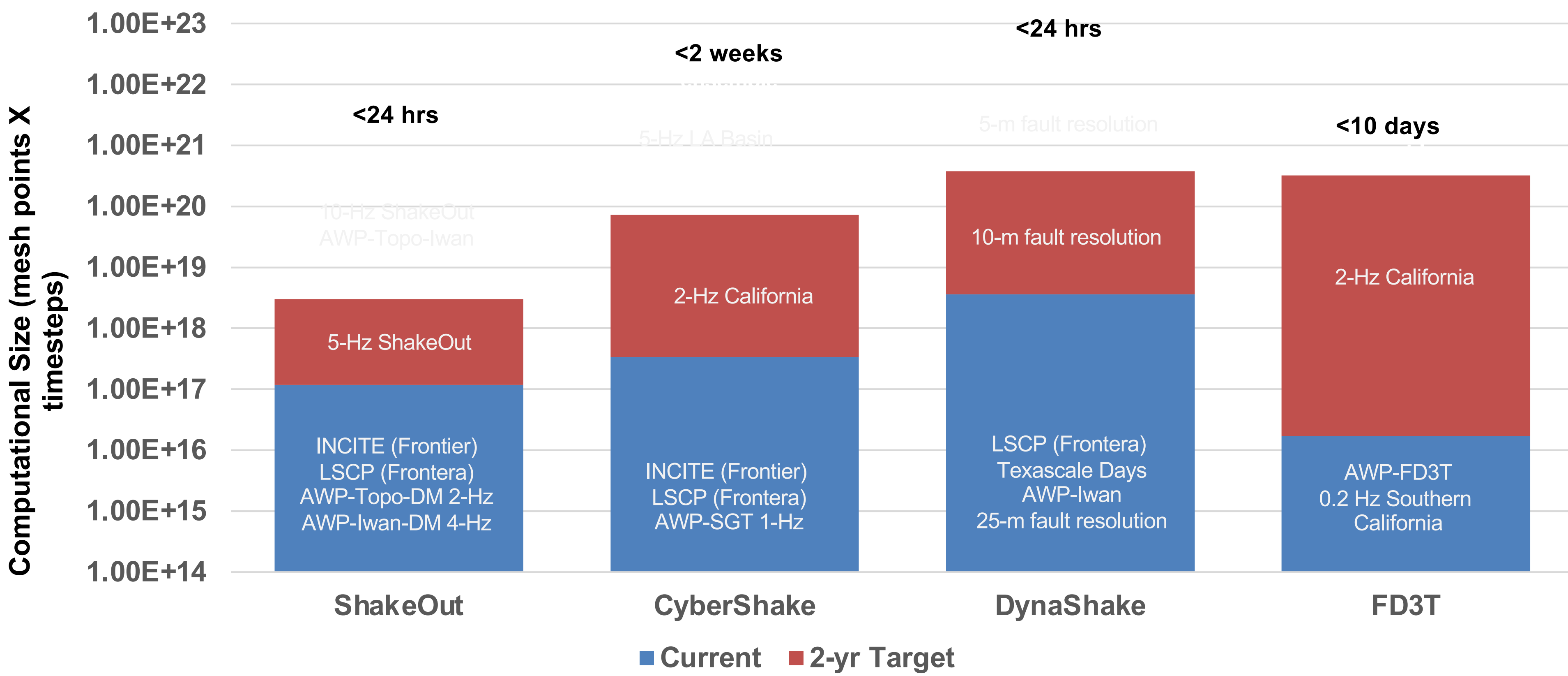

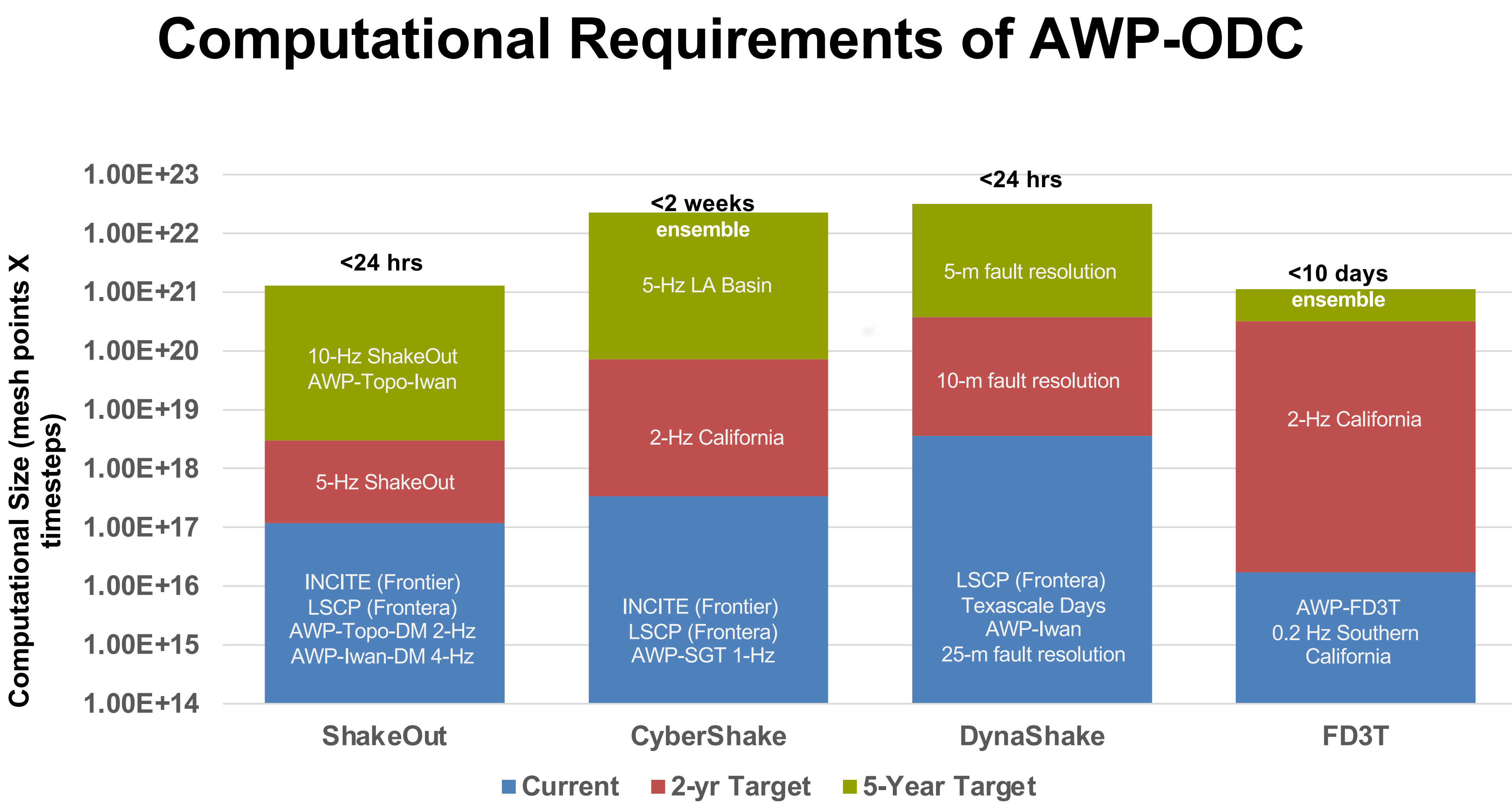
Computational Requirements of AWP-ODC
Computational Size (mesh points X timesteps)
1.00E+23
1.00E+22
1.00E+21
1.00E+20
1.00E+19
1.00E+18
1.00E+17
1.00E+16
1.00E+15
1.00E+14
<24 hrs
10-Hz ShakeOut
AWP-Topo-Iwan
5-Hz ShakeOut
INCITE (Frontier)
LSCP (Frontera)
AWP-Topo-DM 2-Hz
AWP-Iwan-DM 4-Hz
<2 weeks
ensemble
5-Hz LA Basin
2-Hz California
INCITE (Frontier)
LSCP (Frontera)
AWP-SGT 1-Hz
<24 hrs
5-m fault resolution
10-m fault resolution
LSCP (Frontera)
Texascale Days
AWP-Iwan
25-m fault resolution
<10 days
ensemble
2-Hz California
AWP-FD3T
0.2 Hz Southern
California
ShakeOut
CyberShake
DynaShake
FD3T
Current
2-yr Target
5-Year Target

The ShakeOut Scenario

- M7.8 scenario along southern San Andreas Fault (SSAF)
- Best possible science for fault geometry and source rupture characteristics in 2008

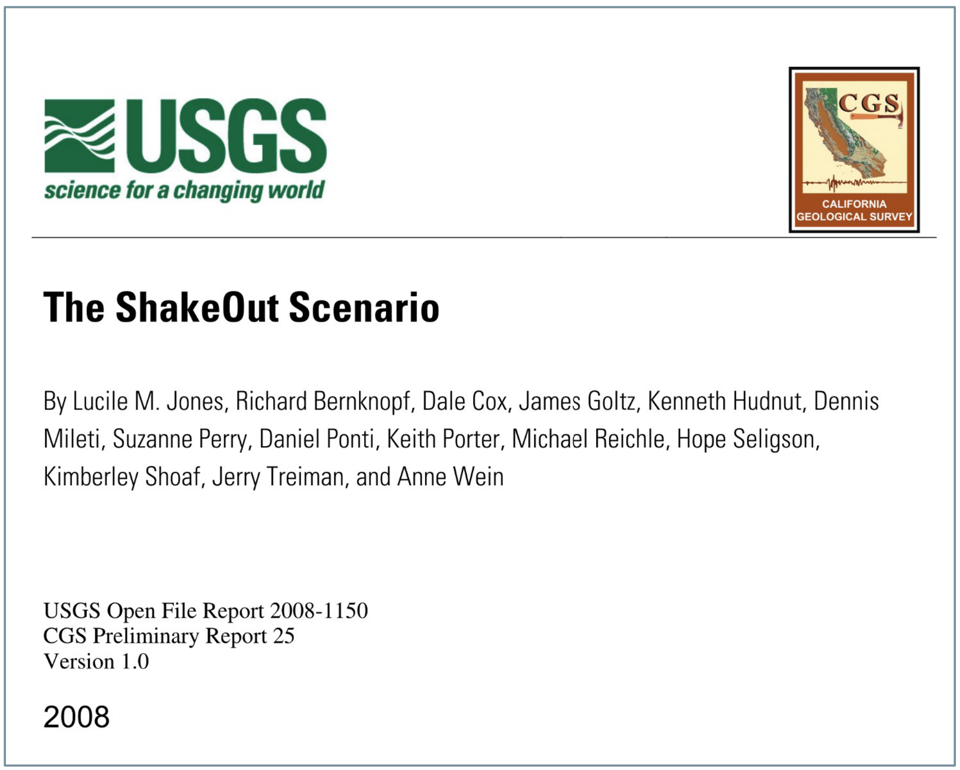
USGS
science for a changing world
CGS
CALIFORNIA GEOLOGICAL SURVEY

The ShakeOut Scenario

By Lucile M. Jones, Richard Bernknopf, Dale Cox, James Goltz, Kenneth Hudnut, Dennis Mileti, Suzanne Perry, Daniel Ponti, Keith Porter, Michael Reichle, Hope Seligson, Kimberley Shoaf, Jerry Treiman, and Anne Wein

USGS Open File Report 2008-1150
CGS Preliminary Report 25
Version 1.0

2008

ShakeOut source model

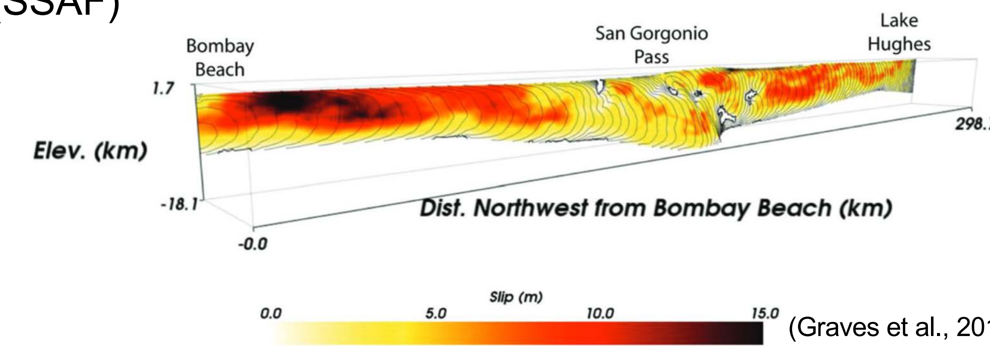

(Graves et al., 2011)

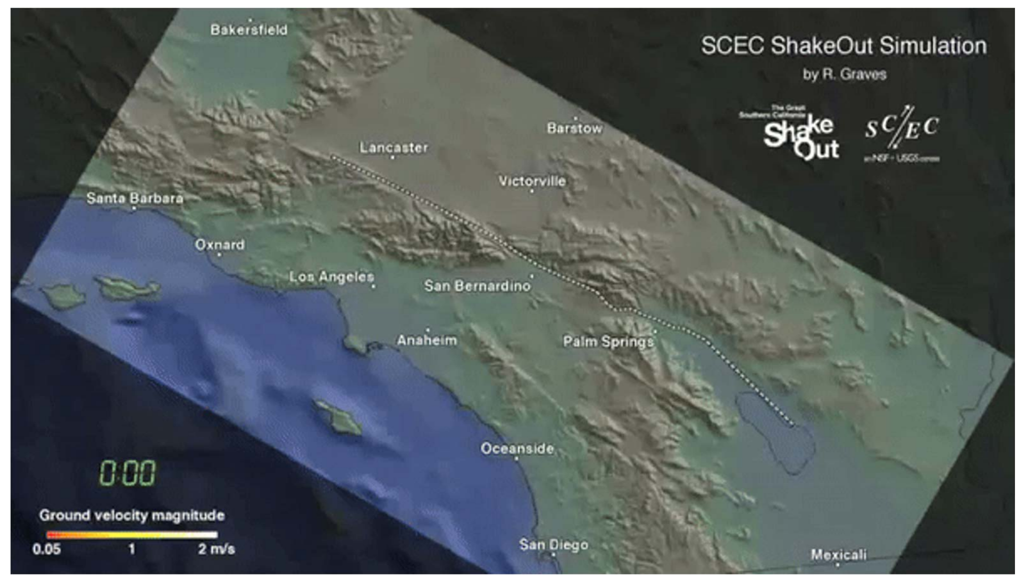

Expected Strong Ground Motions

- Physics-based 3D wave propagation simulation: **AWP-ODC**
- Coherent long-period (3s-period and longer) waveguide channeling into Los Angeles basin
- Is best available science in 2008 still the best?

ShakeOut (Graves et al. 2011)

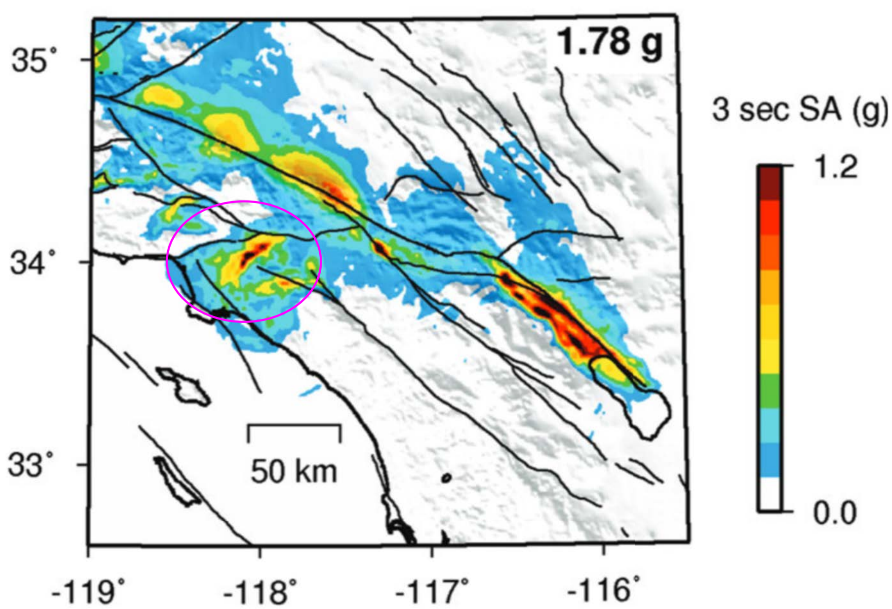

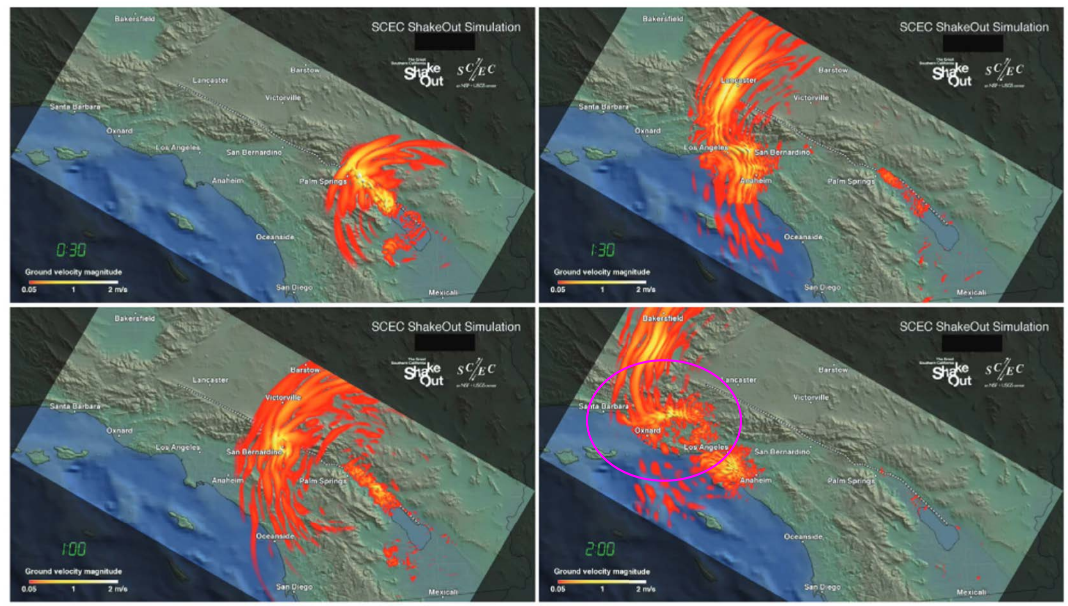

Improved/New Model Features

- Updated Statewide California Earthquake Center (SCEC) Community Velocity Model (CVM):
  Previous: CVM-S4 (Kohler et al., 2003; Magistrale et al., 2000) New: CVM-S4.26.M01 (Lee et al., 2014)

- Surface topography
  Flat vs. Irregular free surface

- Local high-resolution models:
  (1) Imperial Valley (Persaud et al., 2016)
  (2) Coachella Valley (Ajala et al., 2019)
  (3) San Gabriel-Chino-San Bernardino basin (Li et al., 2023)

- High-resolution fault geometry
  Salton Seismic Imaging Project (Fuis et al., 2017)

- Small-scale heterogeneities
  Elastic scattering model (Lin & Jordan, 2023)

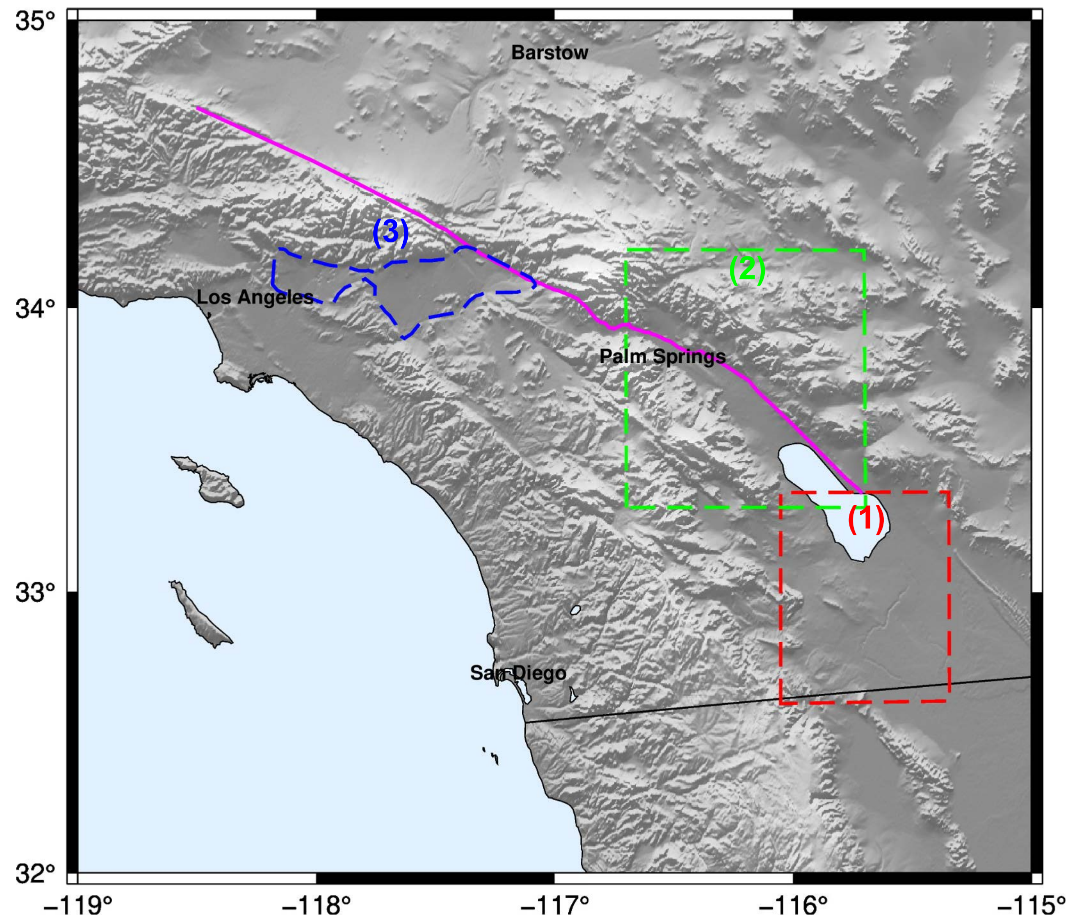

Local Models

(1) Imperial Valley/Coachella Valley models

- Persaud et al. (2016) for Imperial Valley
- Ajala et al. (2019) for Coachella Valley
- Travel time tomography (P-wave)
- SSIP (Salton Seismic Imaging Project) seismic survey

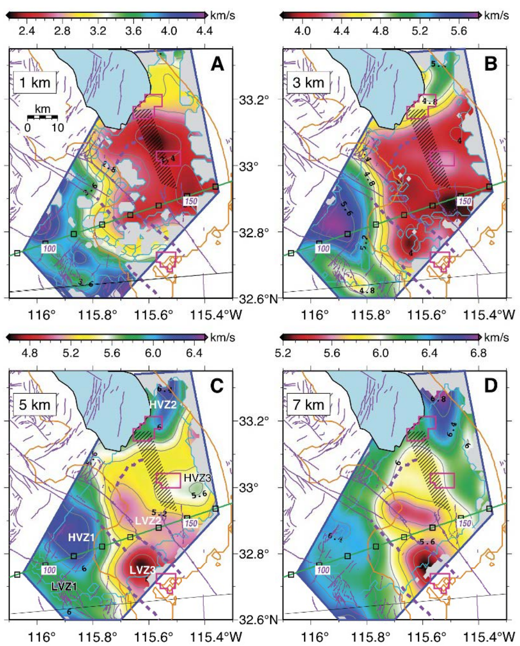

Persaud et al. (2016)

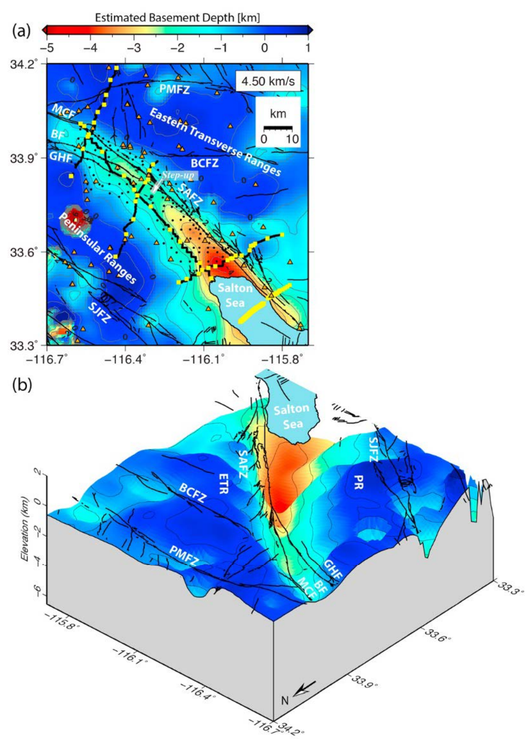

Ajala et al. (2019)

(2) San Gabriel-Chino-San Bernardino basins

- Li et al. (2023)
- Ambient noise tomography using linear arrays

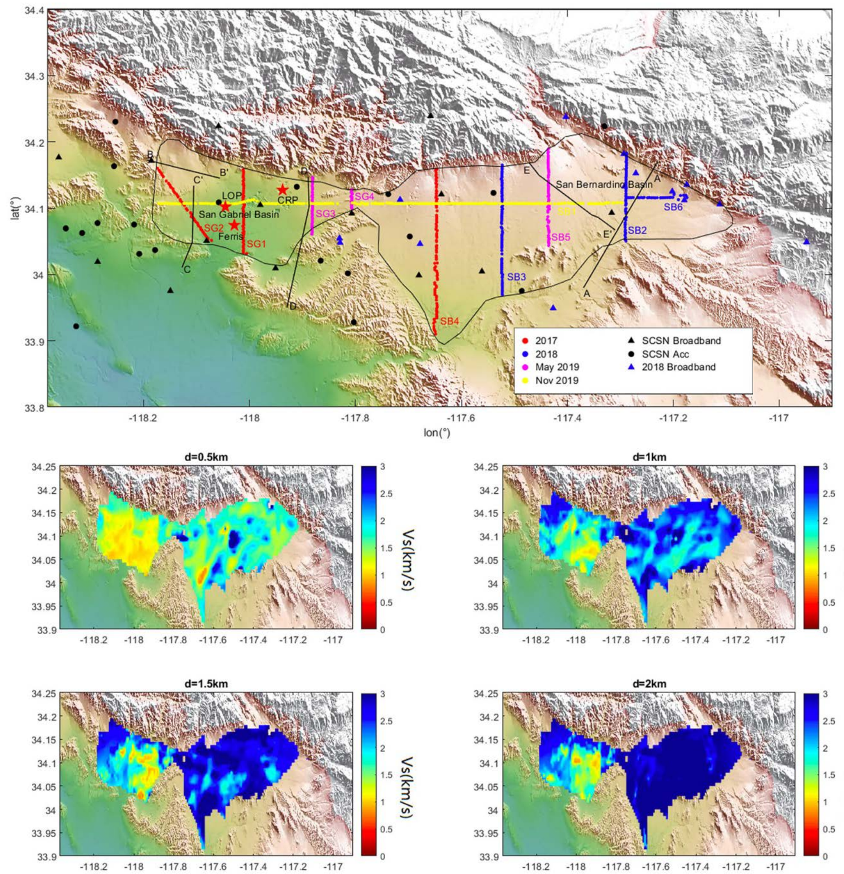

AWP-ODC - Recent Advancements

- GPU-enabled and highly scalable (Cui et al., 2013), with **curvilinear grid** and **discontinuous mesh** features
- Developed and verified on Summit at Oak Ridge Leadership Computing Facility (OLCF), with Nvidia V100 GPUs
- Verified ported HIP version, full production runs on AMD GPU machines (Frontier at OLCF)

Implementation of Curvilinear Transformation

- Implementing traction free boundary using curvilinear grid (O'Reilly et al., 2021)
- Horizontal grid spacing remains
- Vertical grid stretching
- Curvilinear mapping
- Numerical challenge: Staggered-grid finite-difference scheme

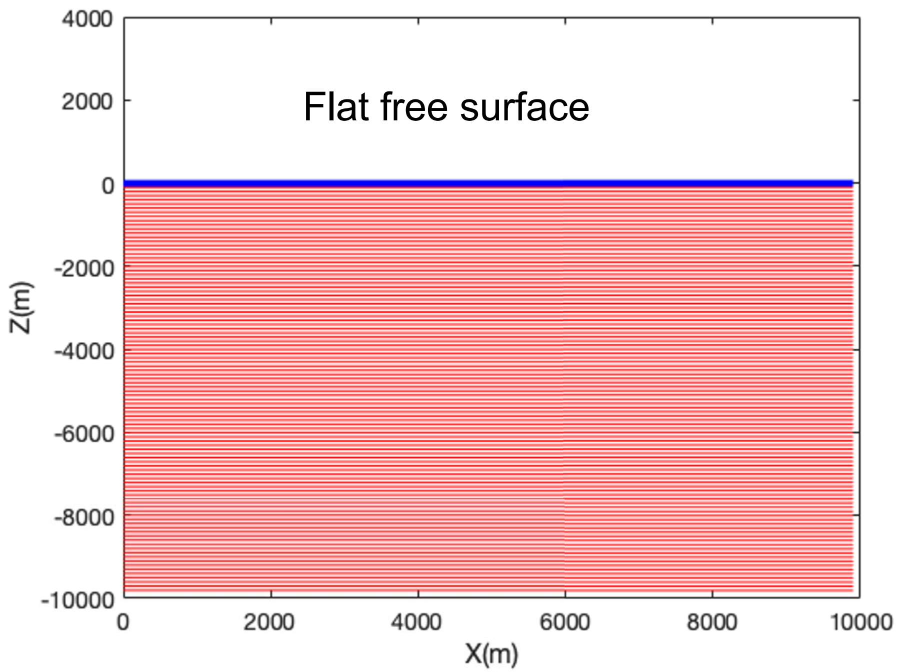

$$x_1 = F_1(r^1, r^2, r^3), \quad x_2 = F_2(r^1, r^2, r^3), \quad x_3 = F_3(r^1, r^2, r^3)$$

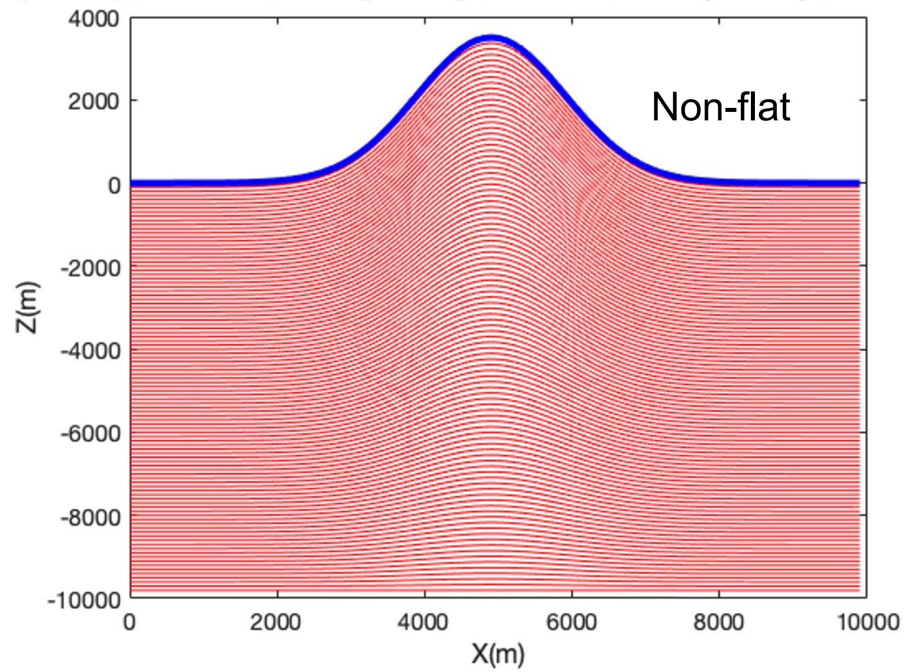

Governing Equations with Curvilinear Grid

Covariant basis vector (tangential):

$$\mathbf{a}_i = \begin{bmatrix} \frac{\partial x_1}{\partial r^i} \\ \frac{\partial x_2}{\partial r^i} \\ \frac{\partial x_3}{\partial r^i} \end{bmatrix}, \quad a_{ij} = \frac{\partial x_j}{\partial r^i}$$

Contravariant basis vector (orthogonal):

$$\mathbf{a}^j = \begin{bmatrix} \frac{\partial r^j}{\partial x_1} \\ \frac{\partial r^j}{\partial x_2} \\ \frac{\partial r^j}{\partial x_3} \end{bmatrix}, \quad a^{ji} = \frac{\partial r^j}{\partial x_i}$$

Establishing orthogonality:

$$\mathbf{a}_i \cdot \mathbf{a}^j = \delta_{ij}$$

Governing equation in Cartesian coordinate:

$$\rho \frac{\partial v_i}{\partial t} = \sum_{j=1}^{3} \frac{\partial \sigma_{ij}}{\partial x_j},$$

$$\frac{\partial \sigma_{ij}}{\partial t} = \lambda \sum_{k=1}^{3} \frac{\partial v_k}{\partial x_k} \delta_{ij} + \mu \left(\frac{\partial v_i}{\partial x_j} + \frac{\partial v_j}{\partial x_i} \right)$$

$$\downarrow$$

$$\boxed{\begin{gathered}\text{Governing equation in curvilinear coordinate:}\\ \rho \frac{\partial v_i}{\partial t} = \frac{1}{J} \sum_{k,j} \frac{\partial}{\partial r^k} (J a^{kj} \sigma_{ij}),\\ \frac{\partial \sigma_{ij}}{\partial t} = \lambda \sum_{k,l} \frac{\partial v_k}{\partial r_l} a^{lk} \delta_{ij} + \mu \sum_{l} \left(\frac{\partial v_i}{\partial r^l} a^{lj} + \frac{\partial v_j}{\partial r^l} a^{li} \right)\end{gathered}}$$

$$\rho\frac{\partial v_i}{\partial t} = \frac{1}{J}\left(\frac{\partial}{r^1}(Ja^{11}\sigma_{i1}) + \frac{\partial}{r^2}(Ja^{21}\sigma_{i1}) + \frac{\partial}{r^3}(Ja^{31}\sigma_{i1})\right)$$
$$+ \frac{1}{J}\left(\frac{\partial}{r^1}(Ja^{12}\sigma_{i2}) + \frac{\partial}{r^2}(Ja^{22}\sigma_{i2}) + \frac{\partial}{r^3}(Ja^{32}\sigma_{i2})\right)$$
$$+ \frac{1}{J}\left(\frac{\partial}{r^1}(Ja^{13}\sigma_{i3}) + \frac{\partial}{r^2}(Ja^{23}\sigma_{i3}) + \frac{\partial}{r^3}(Ja^{33}\sigma_{i3})\right),$$

$$\frac{\partial \sigma_{ij}}{\partial t} = \lambda\left(\left(\frac{\partial v_1}{\partial r_1}a^{11} + \frac{\partial v_1}{\partial r_2}a^{21} + \frac{\partial v_1}{\partial r_3}a^{31}\right)\right.$$
$$+ \left(\frac{\partial v_2}{\partial r_1}a^{12} + \frac{\partial v_2}{\partial r_2}a^{22} + \frac{\partial v_2}{\partial r_3}a^{32}\right)$$
$$\left. + \left(\frac{\partial v_3}{\partial r_1}a^{13} + \frac{\partial v_3}{\partial r_2}a^{23} + \frac{\partial v_3}{\partial r_3}a^{33}\right)\right)\delta_{ij}$$
$$+ \mu\left(\left(\frac{\partial v_i}{\partial r^1}a^{1j} + \frac{\partial v_i}{\partial r^2}a^{2j} + \frac{\partial v_i}{\partial r^3}a^{3j}\right)\right.$$
$$\left. + \left(\frac{\partial v_j}{\partial r^1}a^{1i} + \frac{\partial v_j}{\partial r^2}a^{2i} + \frac{\partial v_j}{\partial r^3}a^{3i}\right)\right).$$

a^{kk} Diagonal terms, easy to implement

$a^{kj},\ k \neq j$ Off-diagonal terms, not so easy, need interpolation

Estimation of velocity and stress components using numerical differencing operator

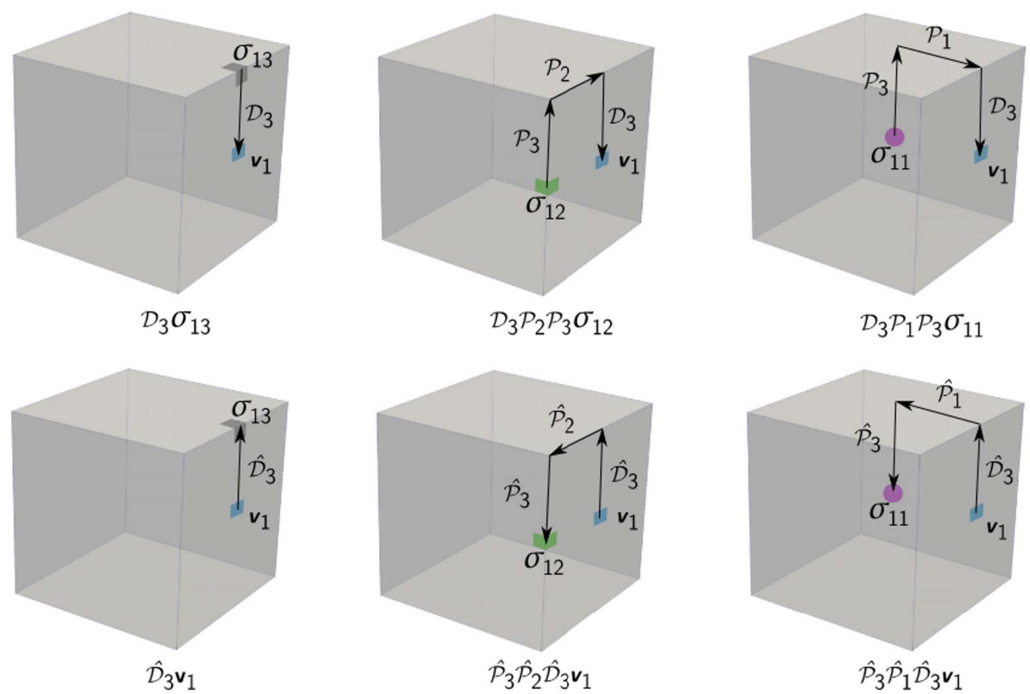

Stability Criterion and Verification

For Cartesian grid, CFL criterion is (4th-order FD):

$$\Delta t < \min \frac{\Delta x}{\sqrt{3} V_p (c_1 + c_2)} = C \min \frac{\Delta x}{V_p} \approx 0.495 \min \frac{\Delta x}{V_p}$$

For curvilinear grid:

$$\Delta t < C_0 \min \frac{\Delta x}{V_p}$$ (Horizontal grid directions or region with little to no grid deformation)

$$\Delta t < C_1 \min \frac{h}{V_p \|\mathbf{a}^3\|_2}$$ (Vertical grid directions with curvilinear transformation)

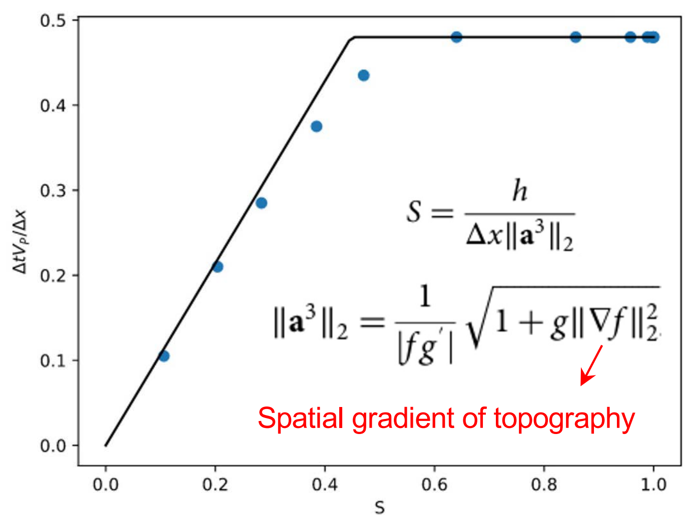

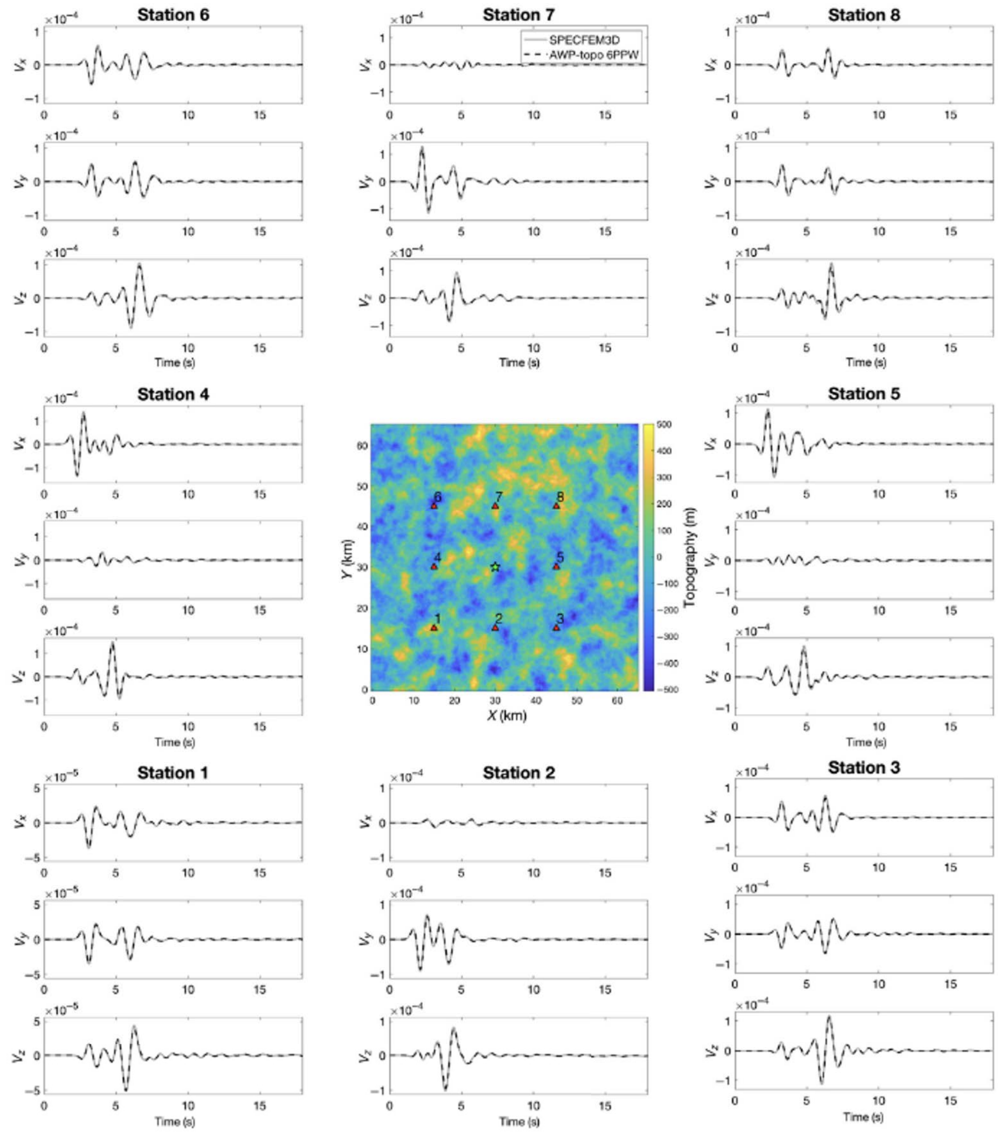

Implementation of Discontinuous Mesh (DM)

- Nie et al. (2017)
- Wavefield Estimation Using a Discontinuous Mesh Interface (WEDMI)
- Overlap zone for data exchange
- Factor-of-three ratio coarsening

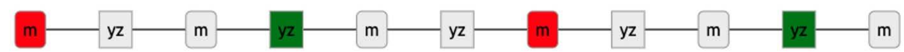

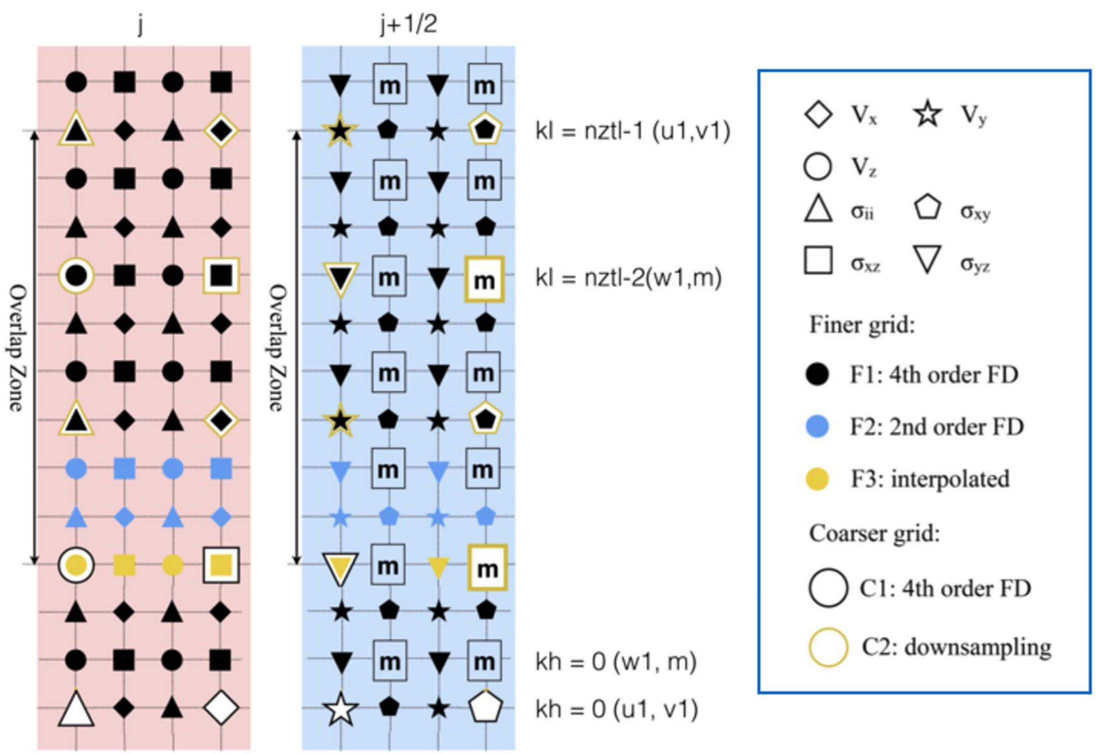

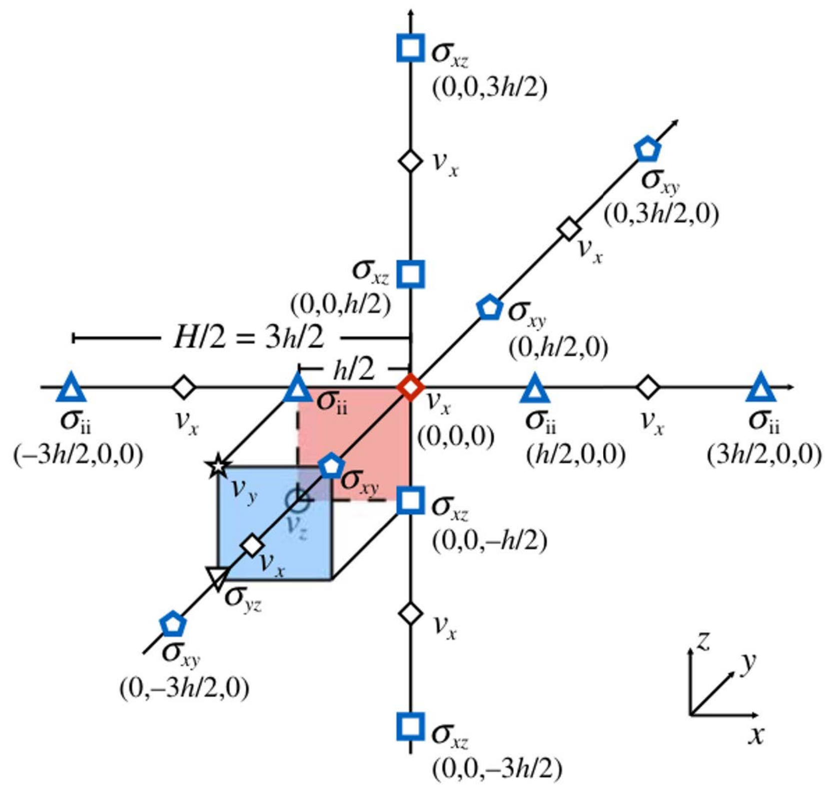

Implementation of Discontinuous Mesh (DM)

- Downsampling process needed
- Directly passing values to collocated coarser grids
  -> proven unstable
- Filter first and interpolated

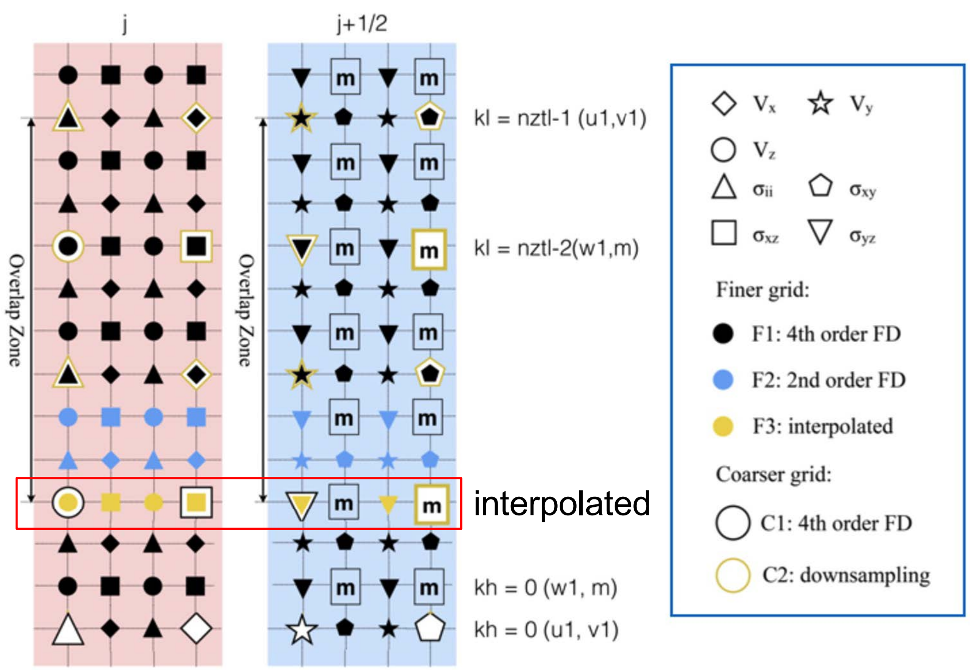

Velocity field update:
1. fourth-order velocities update in the coarser region (C1)
2. fourth-order velocities update in the finer region (F1)
3. second-order velocities update in the finer region (F2)
4. free surface calculation
5. interpolation of velocities in the finer region (F3)
6. downsampling of velocities in the coarser region (C2)

Stress field update:
1. fourth-order stresses update in the coarser region (C1)
2. fourth-order stresses update in the finer region (F1)
3. second-order stresses update in the finer region (F2)
4. interpolation of stresses in the finer region (F3)
5. downsampling of stresses in the coarser region (C2)
6. apply source

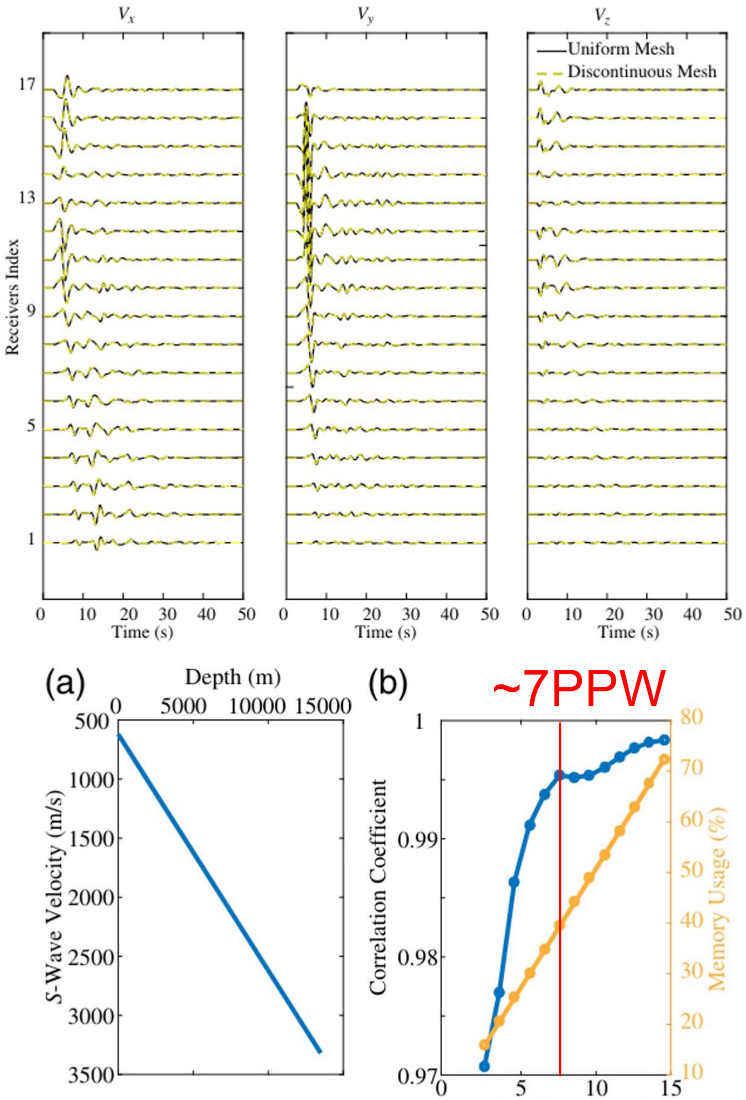

Nie et al. (2017)

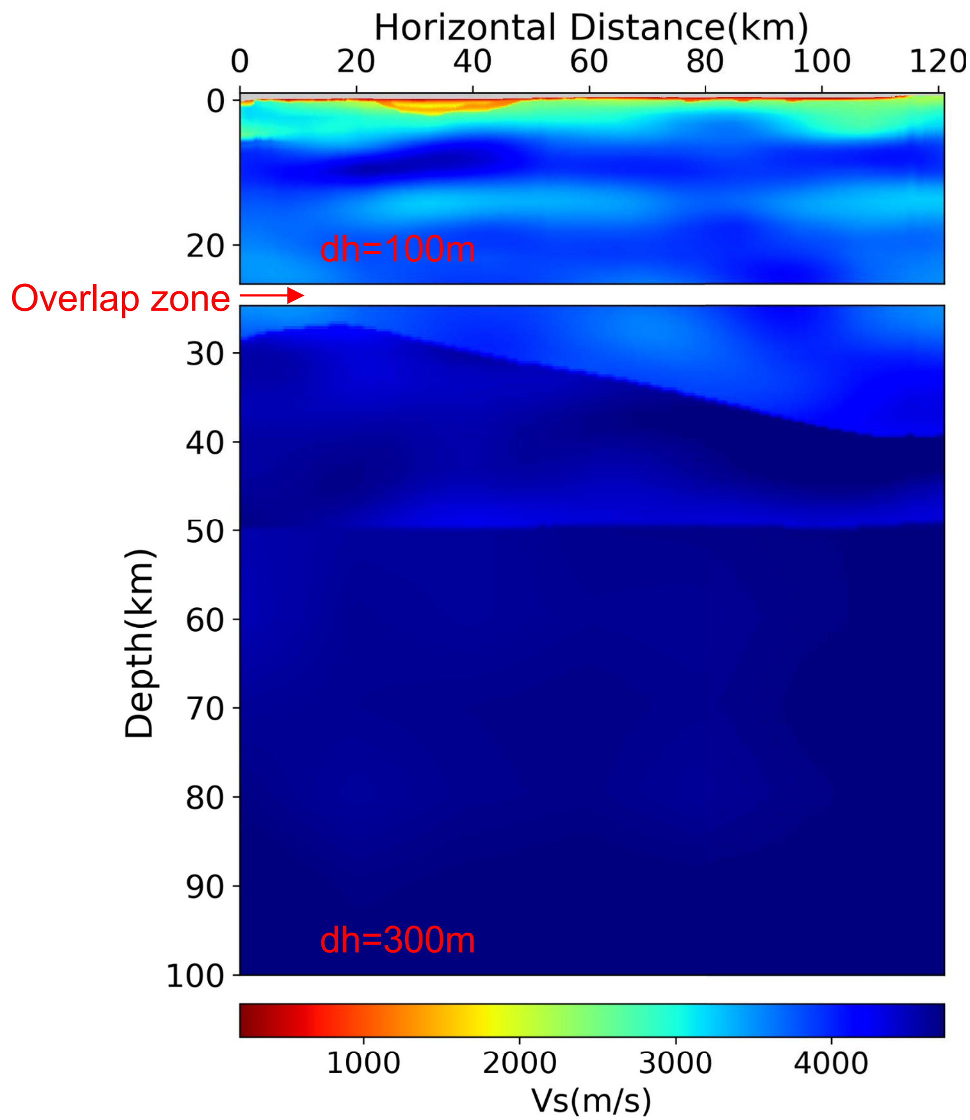

Numerical Models for ShakeOut

- Numerical domain
  1. Following the domain used in earlier ShakeOut studies
  2. 40^0-rotated domain of 600km (Length) x 300 km (Width) with discontinuous mesh
  3. 30m-resolution USGS digital elevation model
  4. Updated attenuation model Qs=**0.1**Vs (versus Qs=0.05Vs used previously)
  5. Minimum Vs of 500 m/s
- Local high-resolution models:
  1. Merged into CVMs using tapering method (Ajala and Persaud, 2021)
  2. Using empirical relations from Brocher (2005) for conversion of required elastic properties

Technical details

Domain	
Length	600 km
Width	300 km
Depth	101.2 km
Southwest corner	$-121.0000^o, 34.5000^o$
Northwest corner	$-118.9520^o, 36.6210^o$
Southeast corner	$-116.0331^o, 31.0835^o$
Northeast corner	$-113.9455^o, 33.1223^o$
Rotation angle	40^o clockwise from north
Geodetic datum	WGS84
UTM zone	11
Spatial resolution	
Maximum frequency	1 Hz
Minimum V_S	500 m/s
Points per minimum wavelength	5
Grid spacing	100 m: Free surface to 25.4 km below sea level 300 m: 24.7 km to 101.2 km below sea level
Temporal resolution	
Time step	0.0045 s
Simulation time	180 s

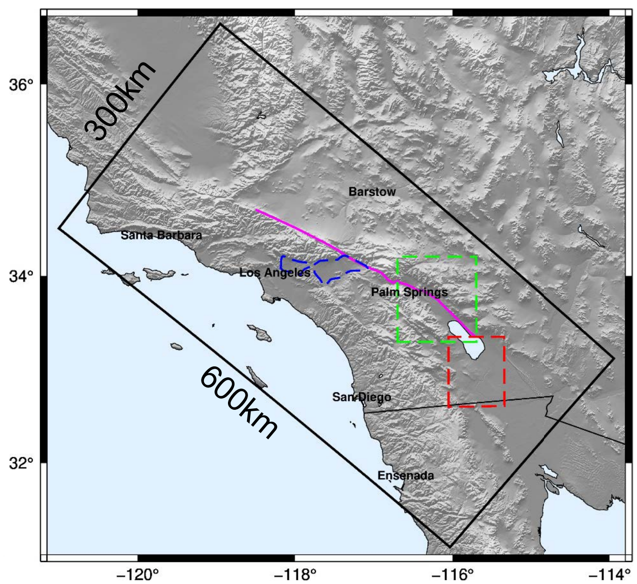

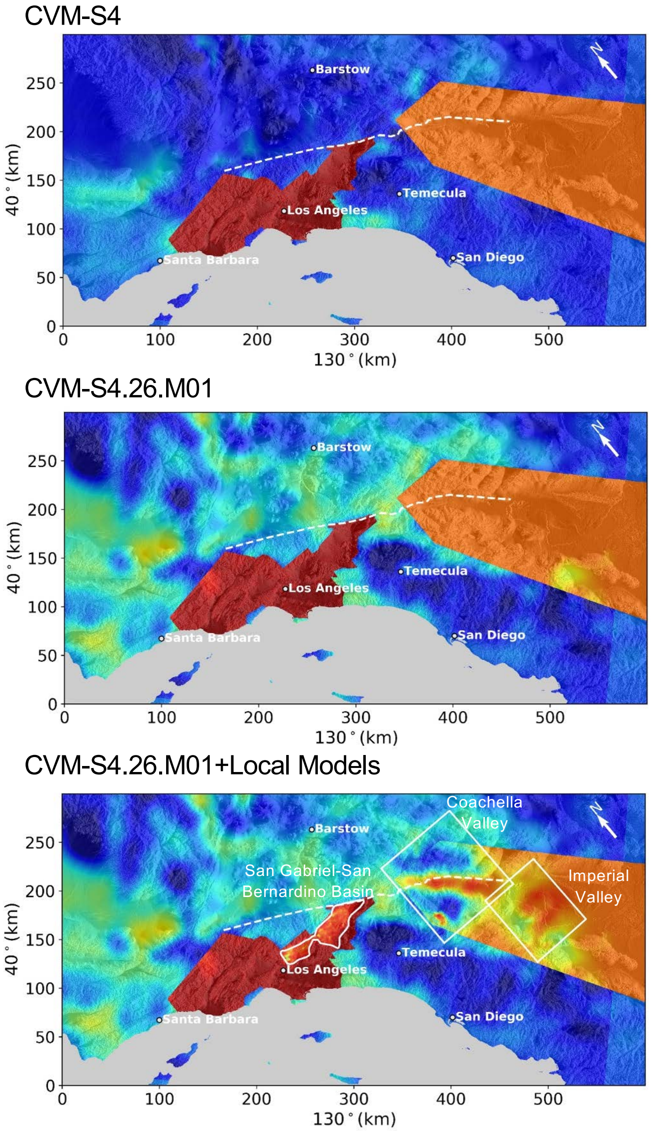

Ground Motions Fade with Model Updates

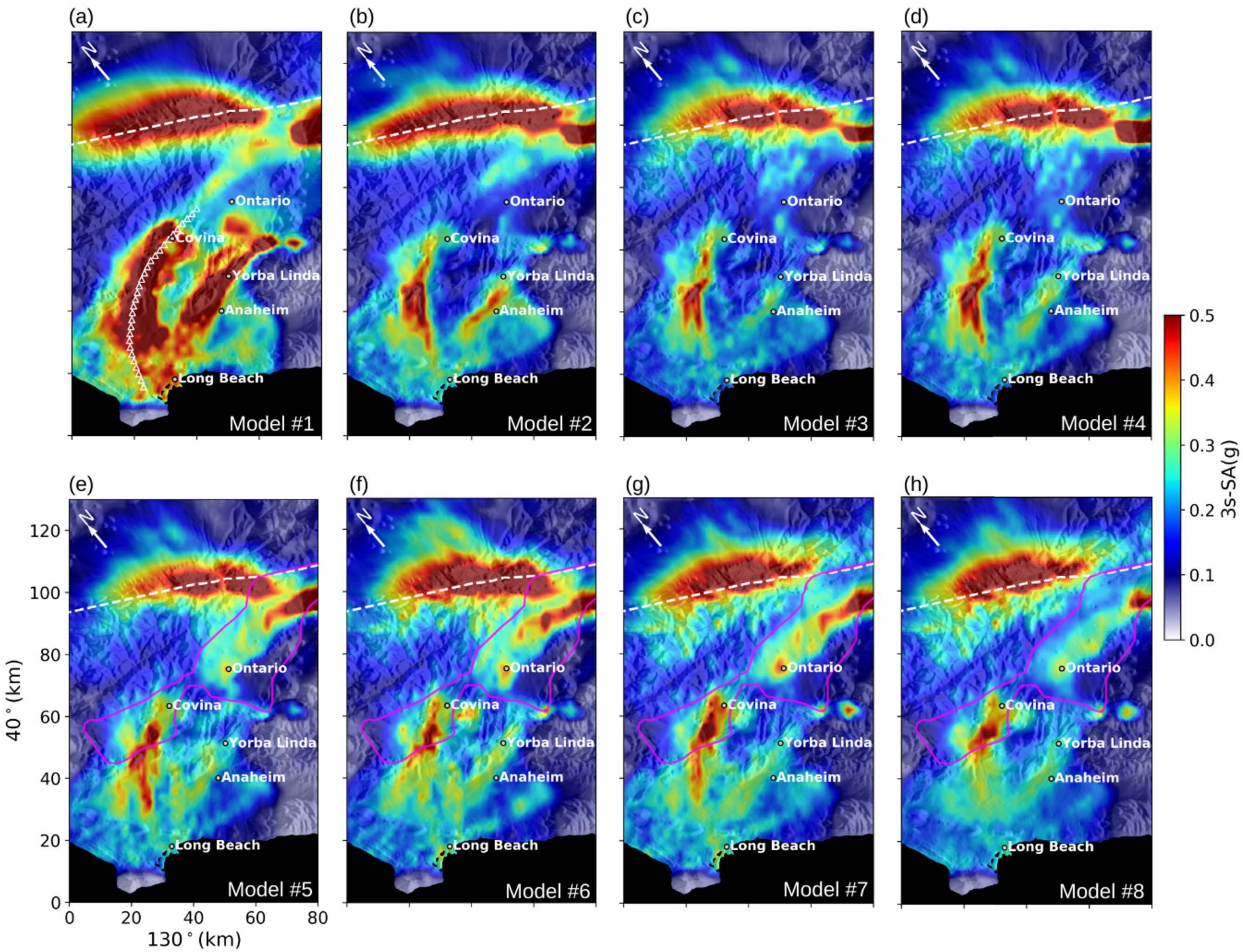

Effects of Model Updates and Surface Topography

- Two branches of waveguides channeling into the LA basin
- Largest reduction (65-100%) occurs when updating reference model
- Adding surface topography leads to smaller reduction (25%) along both waveguide branches, while increasing ground motions in the San Gabriel mountains

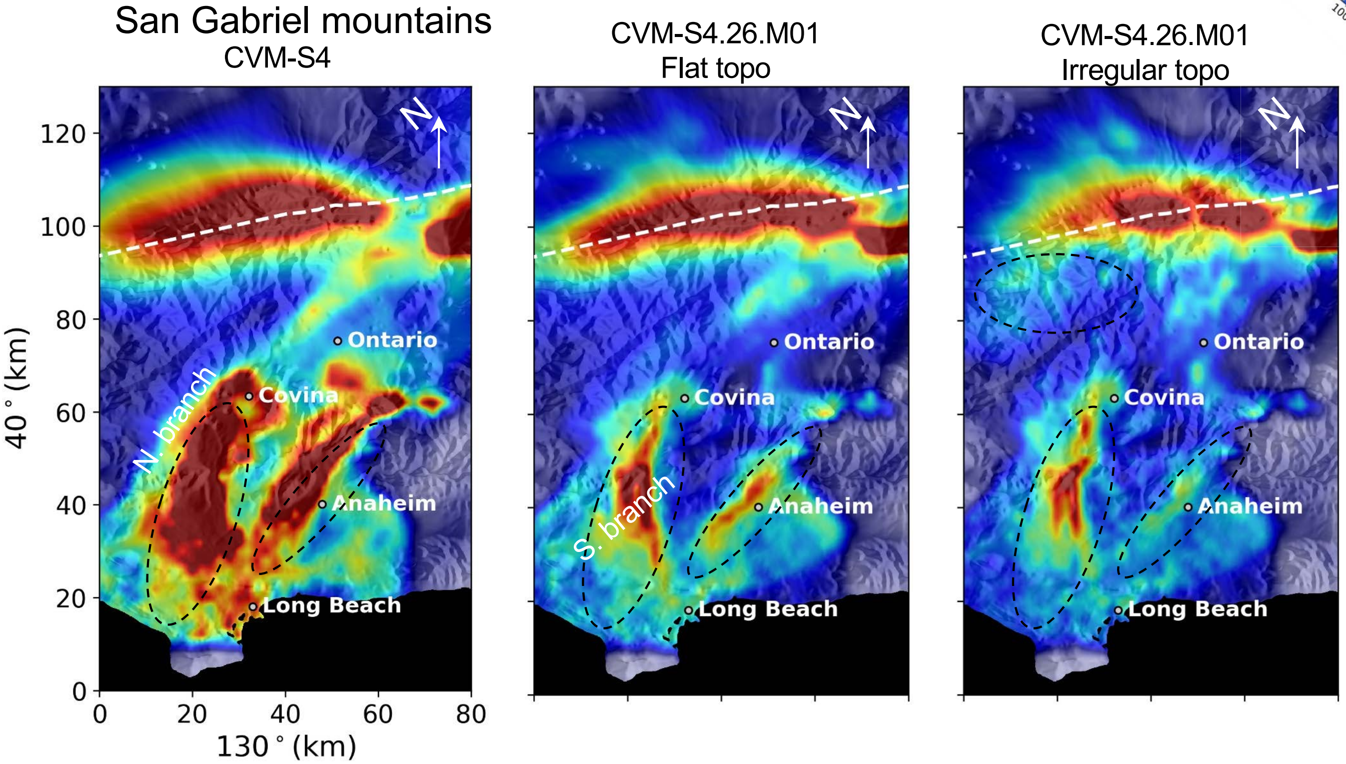

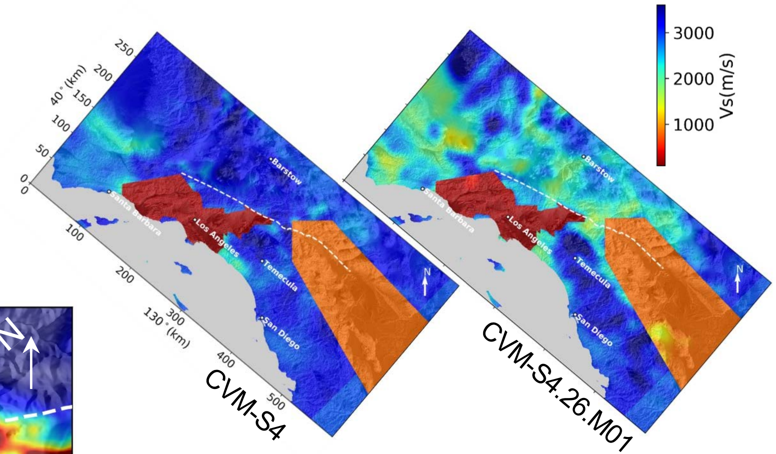

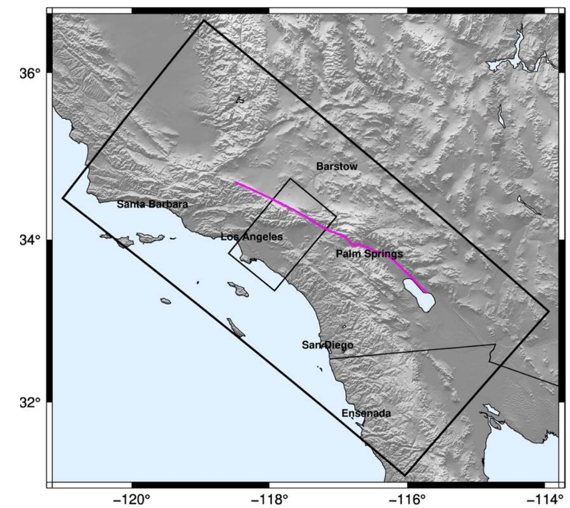

The Final Model...

- The exceptional scalability and performance of the AWP-ODC due to the most recent advancements allows for examination of plenty earth models including the irregular surface topography at low computational cost

- Combining all model features, the predicted ground motions along both waveguide branches are reduced by 50-70% relative to the starting model

- The validation of the final model confirms the robustness of the final model up to 1 Hz.

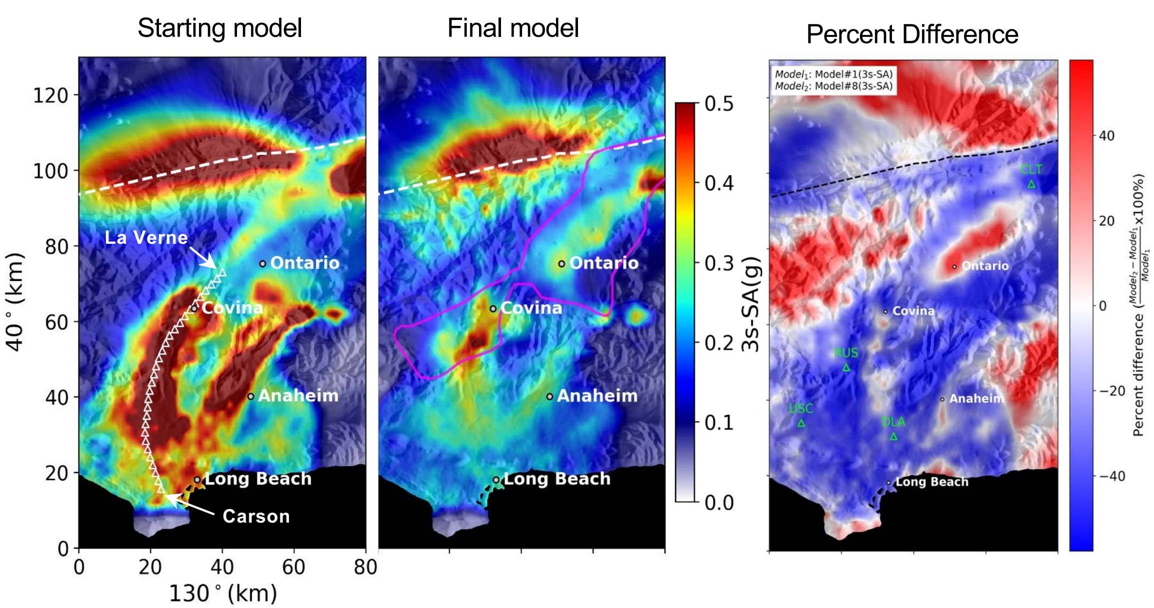

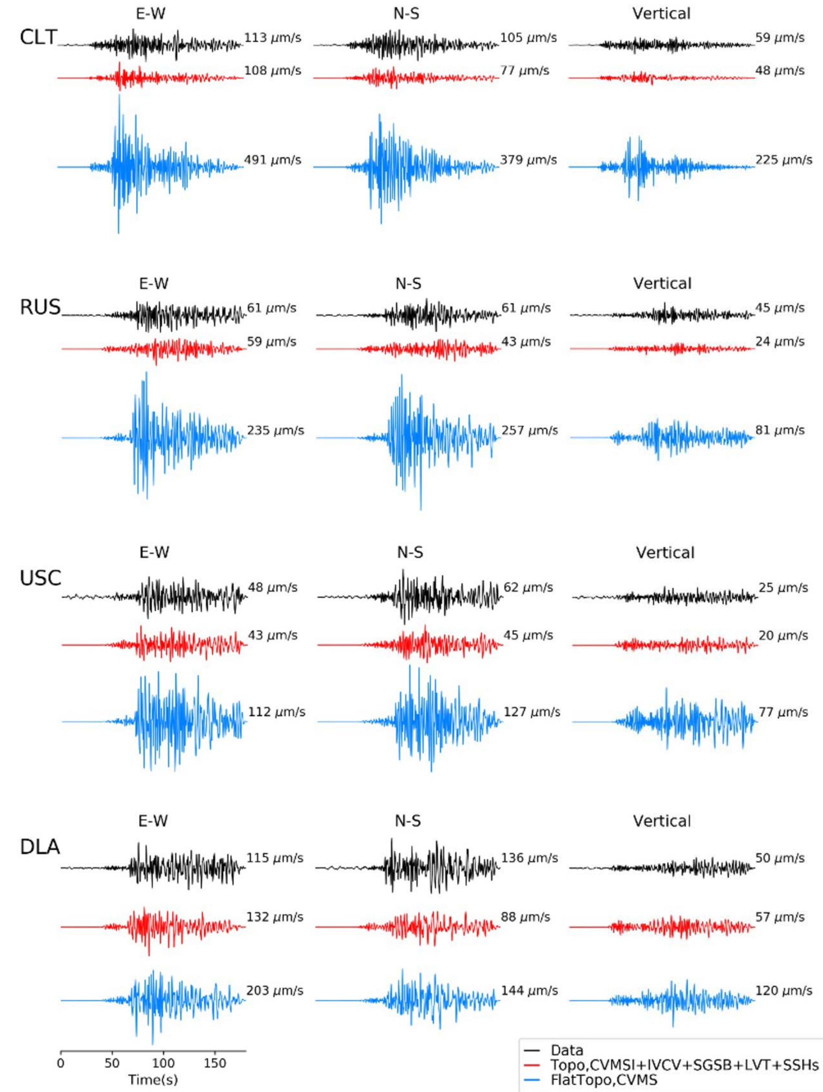

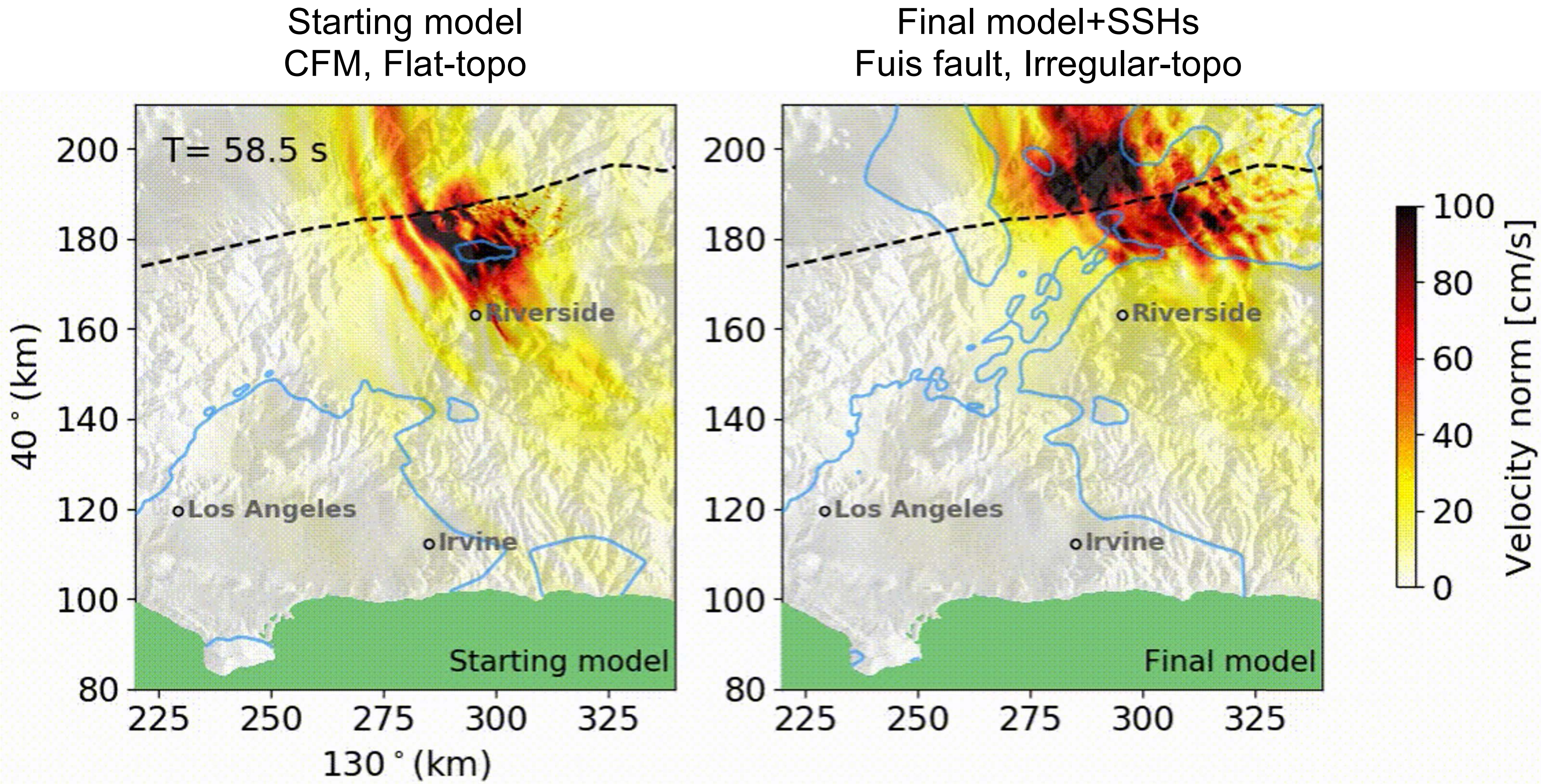

Starting model
CFM, Flat-topo
Final model+SSHs
Fuis fault, Irregular-topo
T= 58.5 s
Riverside
Los Angeles
Irvine
Starting model
Final model
40° (km)
130° (km)
200
180
160
140
120
100
80
225
250
275
300
325
Velocity norm [cm/s]
100
80
60
40
20
0